The Molecular Mechanism of Membrane Proteins Probed by Evanescent Infrared Waves

Rebecca M. Nyquist, Kenichi Ataka, and Joachim Heberle*[a]

The catalytic action of membrane proteins is vital to many cellular processes. Yet the molecular mechanisms remain poorly understood. We describe here the technique of evanescent infrared difference spectroscopy as a tool to decipher the structural changes associated with the enzymatic action of membrane proteins. Functional changes as minute as the protonation state of individual amino acid side chains can be observed and linked to interactions with a ligand, agonist, effector, or redox partner.

1. Introduction

Many fundamental cellular processes such as transport, signaling, adhesion, motility, and energy transduction involve integral membrane proteins. The functional prominence of membrane proteins renders them favored targets in pharmaceutical design and warrants a thorough basic understanding of the way they work at the molecular level. Understanding of the physiological mechanism of a membrane protein emerges from structural details about key intermediate steps of enzymatic action. Progress has been impeded by difficulties in nearly every step, from heterologous expression and isolation to crystallization difficulties that arise from the constraints posed by their amphiphilic character.[1] The advent of novel crystallization methods targeted specifically at membrane proteins has spurred success in their crystallography.[2–4] Yet, many of the important structural changes associated with the catalytic mechanism, such as protonation-state changes of individual amino acid side chains, often remain unresolved in the crystallographic models. Therefore, an alternative technique must be used in conjunction with crystallography to gain information about the coordinated involvement of particular residues and the chronological sequence of steps spanning the protein mechanism. Infrared difference spectroscopy is such a technique and, when integrated with the use of evanescent radiation, provides unique capabilities to reveal specific structural changes associated with membrane-protein function. In the following sections, the principles of this technique and its implementation are discussed.

2. Infrared Difference Spectroscopy

IR radiation absorbed by molecules excites oscillatory motions of the nuclei. These excited vibrational motions of groups of atoms are called *vibrational modes*. The frequency of a vibrational mode depends on the mass of the atoms involved and the nature of the bonds connecting them. The frequency of particular vibrations is often modulated by minute changes in the environment surrounding the group, lending acute sensitivity to IR spectroscopy.

The examination of membrane proteins with infrared spectroscopy is a particularly exacting task, and surmounting the various challenges has been a major accomplishment spanning the past 20 years. Most membrane proteins contain sufficient atoms to give rise to approximately 10^4 vibrational modes. In addition to the modes arising from the peptide backbone and the amino acid side chains, there can be contributions from chromophores or cofactors as well as water, buffer, lipids, and detergent molecules present in the sample. Ultimately, this is an intractable number of overlapping vibrational bands that complicates the process of extracting details about the role of individual groups involved in the molecular mechanism. This task is simplified by the use of *difference* spectroscopy (reviewed in refs. [5 – 8]), which examines the differences in absorbance before and after inducing a perturbation that alters the state of the protein, usually simulating part of the physiological reaction that produces an intermediate state. This reaction alters a subset of the total vibrations; only those vibrations altered in the transition appear in the difference spectrum. Resulting changes to the absorbance spectrum can be less than 0.1 % of the total absorbance.

Thus, IR difference spectra represent the molecular vibrations of the protein that become altered in the transition between states. Figure 1 schematically illustrates the shapes of difference band features and how they arise from the absorbance spectra of the individual states. A negative band in the difference spectrum reflects a particular molecular vibration that is *present* in the initial state but *absent* in the intermediate state due to changes in either the chemical nature of that bond or its environment. This scenario is exemplified in Figure 1 A by the deprotonation of a carboxylic acid group, from for example, an aspartic or glutamic acid residue. The carbonyl stretch of the protonated carboxylic acid disappears from the spectral region shown upon deprotonation in the intermediate state. By contrast, when the strength of a hydrogen bond is modulated, the resulting spectral shapes resemble those shown in Figure 1 B.

[a] *R. M. Nyquist, K. Ataka, Priv.-Doz. Dr. J. Heberle*
Forschungszentrum Jülich, IBI-2: Structural Biology
52425 Jülich (Germany)
Fax: (+49) 246-161-2020
E-mail: j.heberle@fz-juelich.de

 DOI: 10.1002/cbic.200300687

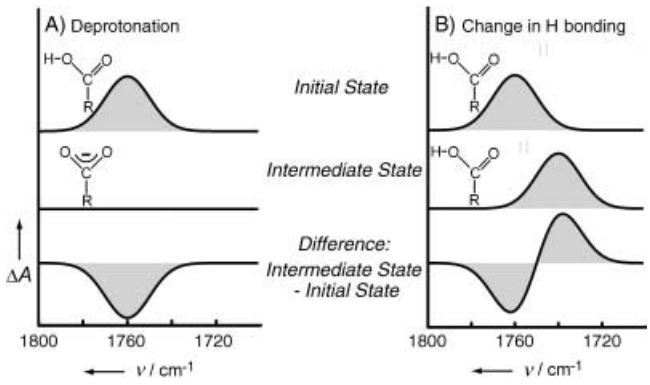

Figure 1. *The origin of IR difference spectral shapes for the transition from an initial state to an intermediate state, exemplified by using a carboxylic acid moiety, for example, from an aspartic or glutamic acid side chain. A) The transition from initial to intermediate state can effect a deprotonation. In the initial state of the protein (top), a distinctive peak arises from the absorbance of the C=O stretching vibration of the protonated carboxylic acid side chain. In the intermediate state of the protein (middle), the peak is absent. The resulting difference spectrum (bottom) shows a negative band. B) The initial to intermediate state transition can change the strength of the hydrogen bonds engaging the carboxylic acid moiety without deprotonation taking place. In the initial state of the protein (top), the distinctive peak arising from the absorbance of the C=O stretch of the protonated carboxylic acid side chain occurs at a particular frequency. In the intermediate state of the protein (middle), the peak is shifted to another frequency (here to lower frequency due to stronger hydrogen bonding). The resulting difference spectrum (bottom) is sinusoidal.*

Often two or more processes are coupled, giving rise to more complex shapes.

The IR difference spectrum contains information about specific structural changes to individual residues of the protein. In order to extract this information, the vibrational bands must be identified. Although the IR difference spectrum is greatly simplified compared with the absorbance spectrum, the assignment of each feature in the spectrum is still a formidable task. Some amino acid vibrations prove relatively easy to recognize. Aspartic and glutamic acids, for example, have a C=O vibration of the COOH side chain appearing in a region that is free of most other overlapping bands.[9] For this reason, the identification of key carboxylic acid amino acids receives marked attention in IR protein studies. Tyrosine also has a rather distinctive vibrational signature.[10] Other amino acids give rise to bands that are much more difficult to identify. Histidine, for example, has bands that are both overlapped by a wide variety of others and also weak in intensity.

Often the location and role of an amino acid implicated in a molecular mechanism can be identified by comparing the IR difference spectra of a protein altered by site-directed mutagenesis and the wild-type protein. When a putative active residue of the protein is altered, the mutant's resulting IR difference spectrum may show specific bands that vanish or shift in comparison to the wild-type's IR difference spectrum. In ideal cases, the shifted or vanished bands arise only from the targeted side chain. In less than ideal cases, however, these also result from changes to the overall protein structure caused by the mutation. Such occurrences can be minimized through the use of conservative mutations, that is, those that replace the native amino acid with one whose side chain preserves as closely as possible the properties of the original residue.

Another band assignment strategy is the use of isotopically labeled amino acid side chains to identify bands that arise from specific amino acids. Replacement of an atom in a molecule by its isotope leads to a frequency shift of the vibrational modes involving that atom. These frequency shifts can help discriminate the bands through a comparison of difference spectra for isotopically labeled and unlabeled protein. There are several ways that isotopes can be introduced into proteins. The solvent-accessible protons within a membrane protein can be changed to deuterons by replacing the water in the sample with D_2O. In membrane proteins expressed in bacterial systems, all one type of amino acid within the protein can be labeled with ^{13}C or ^{15}N by raising the bacteria in growth medium enriched in the isotopically labeled amino acid.[11] The resulting protein then has each occurrence of that amino acid isotopically labeled. In the IR difference spectra, all bands due to that type of amino acid become altered relative to the unlabeled spectra. Isotope labeling and site-directed mutagenesis therefore often make a powerful tool when combined. With all of one kind of amino acid labeled throughout the protein, IR spectral shifts are observed for certain features. When these same shifted features also disappear in the difference spectrum of the mutant protein, the bands can be attributed to the targeted residue. One example of a successful use of this method is the identification the role of two redox-active tyrosines in Photosystem II,[12, 13] a photosynthetic protein. The combination of the global isotopic labeling of tyrosines and the site-directed mutation of both the individual tyrosines and neighboring amino acids hydrogen bonded to them resulted in assignment of bands in the redox difference spectrum.

3. The Advantages of Using Evanescent Waves

Most commonly, IR spectroscopy is performed in the transmission configuration, in which the IR radiation passes directly through the sample. Membrane protein samples require water to be present, and the strong water absorbance obscures too much of the IR spectrum. One way of circumventing this problem is the application of the attenuated total reflection (ATR) technique (Figure 2 left). When the IR radiation is passed through an IR transmissive crystal material, called an *internal reflection element* (IRE), at greater than the critical angle, it is totally internally reflected. A sample applied to the surface of this IRE receives IR radiation from evanescent (i.e., slowly fading away) waves generated at the interface between the (optically denser) IRE and the (optically rarer) sample.[14] These evanescent waves provide the IR energy to excite the vibrations of the sample. The decay of the intensity of the wave is exponential. The depth to which the evanescent waves penetrate the sample is characterized by the distance at which the intensity has decayed to $1/e$:

$$d_p = \frac{\lambda/n_1}{2\pi[\sin^2\Theta - (n_2/n_1)^2]^{1/2}} \quad (1)$$

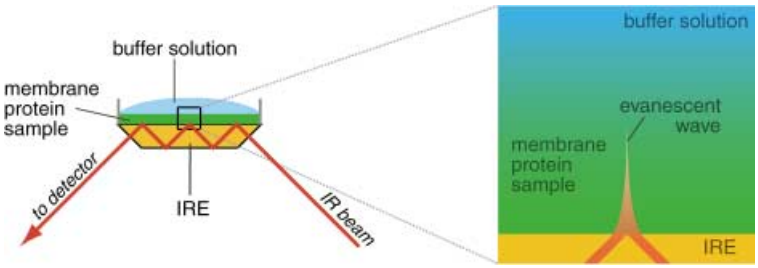

Figure 2. *The geometric configuration of the path of the infrared radiation through the membrane protein sample. The IR beam is totally internally reflected through an internal reflection element (IRE). The membrane protein sample rests on this IRE and has a different index of refraction. This index of refraction mismatch results in some of the IR radiation leaking into the sample as an evanescent wave. This evanescent-wave IR radiation is used to excite the molecular vibrations of the membrane protein samples. A buffer solution bathing the sample can be exchanged for one of different pH, ionic strength, or chemical composition. The schematic enlargement illustrates the penetration of the evanescent wave, which decays exponentially from the surface of the IRE. The protein film (green) is generally much thicker than the penetration depth of the evanescent wave (fading orange), and consequently, the wave does not extend into the buffer solution (blue) bathing the sample, thereby avoiding the problem of strong absorption of water.*

Here d_p = penetration depth, λ = wavelength, n_1 = refraction index of the IRE, n_2 = refraction index of the sample, and Θ = angle of incidence. By using an angle of incidence of 45°, ZnSe or diamond as IRE, and water as sample, a penetration depth of 1.6 μm is calculated from the above formula ($\lambda = 10^{-5}$ m). If the physical dimensions of the IRE are chosen such that six internal reflections are used, an effective path length of 10 μm results. This is comparable to the path length of commonly used transmission cells with the significant advantage that the path length is always constant in ATR experiments.

The above description is rather simplifying, and the calculation is meant to provide the experimentalist with a practical gauge. The physical basis of evanescent waves is far more complex and hence beyond the scope of this article. For greater detail surrounding the physical aspects of evanescent waves, the reader is referred to excellent treatments of this topic.[14–16]

If a sample is enriched at the surface of the IRE, only the sample material is probed by the evanescent wave, provided sample thickness is larger than the penetration depth of radiation (Figure 2 right). Sample enrichment is usually achieved by gently drying a concentrated membrane suspension on the surface of the IRE. Under appropriate conditions (ionic strength and pH) the resulting film does not dissolve when rewetted with an aqueous solution. Water penetrates in between the membrane layers, swelling the stack.[17] This swelling process can be monitored in situ, and therefore the point at which long-term stability of the hydrated membrane stack is reached can be verified. Other methods of achieving sample enrichment within the evanescent wave are the use of self-assembled monolayers (SAMs)[18] or covalent binding of the sample to the surface of the IRE.[19]

ATR/FTIR has long been commonly used in material science and industrial applications.[20–22] The technique is, however, particularly well suited to resolving some of the difficulties surrounding the examination of membrane proteins. The great advantage of using evanescent waves lies in the reservoir of aqueous buffer. This can be exchanged for another solution of differing pH or chemical composition. This possibility of perfusion exchange permits spectra of the same sample to be recorded under a wide variety of solution conditions. However, the exchange process must not alter the protein concentration within the penetration depth of the evanescent wave. The sample must be prepared in such a way that it is adhesive to the IRE and can withstand exchange of the solution. Membrane proteins are naturally well suited for adhesion to the IRE; some can be purified with their natural lipids, facilitating their adhesion to the IRE. Other membrane proteins are purified in detergent, which does not adhere to the IRE. In such cases, detergent can be removed or exchanged for lipid[23] in order to make the protein sample adhesive to the IRE.

4. Applications

Evanescent-wave IR spectroscopy has been widely used to estimate the secondary structure of membrane proteins.[16] This is an old technique that has become a standard in many cases. However, only in a few cases has ATR/FTIR difference spectroscopy been employed to identify the role of specific residues in the molecular mechanism of membrane proteins. Summarized here are examples from four membrane proteins for which key molecular mechanistic details have been gathered from this technique.

4.1. Bacteriorhodopsin: A prototypical proton pump

Bacteriorhodopsin is a haloarcheal membrane protein that absorbs photons and uses the energy to pump protons out of the cytoplasm.[24] Under oxygen-poor environmental conditions, the resulting electrochemical gradient is used for the synthesis of ATP. Although several chief mechanistic details remain unresolved, bacteriorhodopsin is one of the best-understood membrane protein. For this reason, it is regarded as a model for proton pumps, photosynthetic proteins, and G-protein coupled receptors. Bacteriorhodopsin (bR, Figure 3 A) lends itself particularly well to evanescent-wave IR difference spectroscopy because it is purified with its native membrane facilitating the adherence to the surface of the IRE for recording IR difference spectra of the catalytic reaction cycle with the ATR sampling technique.[17] The physiological reaction of bR can be triggered with a laser pulse and it is cyclic; this allows for techniques to be applied that require repetitive excitation of the enzymatic reaction. Although the number of IR photons is significantly lower with reflection spectroscopy than in conventional transmission spectroscopy, IR difference absorption spectroscopy can still be performed with the ATR technique, even with a time resolution as high as 5 μs, by the integration of step-scan spectroscopy.[17] A clear-cut kinetic separation of the photocycle intermediates of bR was achieved by the controlled variation of the pH of the aqueous solution in which the sample had been immersed.[25] The clean representation of the IR difference spectrum of a specific intermediate without contributions from

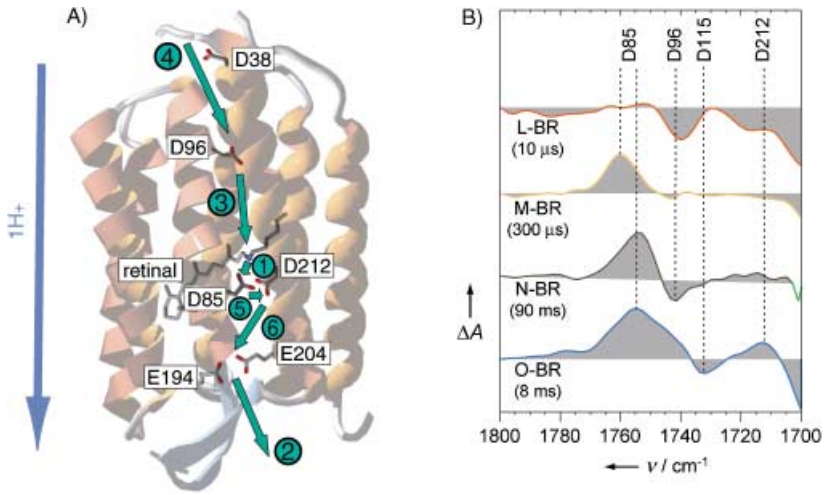

Figure 3. *A) Crystallographic model of the three-dimensional structure of bacteriorhodopsin (PDB entry: 1C3W). The green arrows denote proton-transfer reactions taking place between particular amino acids and the retinal. The circled numbers indicate the sequence of the proton-transfer steps. B) Time-resolved ATR/FTIR difference spectra in the carbonyl region of the photoreaction of bacteriorhodopsin. The difference spectra of the respective intermediate states (L, M, N, and O versus bR) were recorded under different environmental conditions to obtain clean difference spectra without contributions from other intermediate states (see ref. [25] for further details). The band assignment (dashed lines) illustrates the transient acid/base reactions of particular amino acids along with the environmental changes in the vicinity of the respective carboxylic acid. Negative bands are due to the deprotonation of an aspartic acid whereas protonation is indicated by a positive band.*

other intermediates is crucial for the assignment of vibrational changes to certain reaction steps. Single proton transfer events can be deciphered from the carbonyl region (Figure 3B) along with their temporal sequence as determined by time-resolved experiments. These results complement those obtained with the conventional transmission technique,[26, 26] especially in the ground-breaking experiments performed by the Gerwert group.[28]

The pK_a of amino acid side chains is assessed by pH-induced IR difference spectroscopy in the ATR mode.[29, 30] Moreover, time-resolved ATR/FTIR spectroscopy at various pH values leads to the quantitative determination of the dynamic change in pK_a of the critical aspartatic acid, D96.[31] The apparent pK_a of the carboxylic side chain has been shown to decrease from an apparent pK_a of greater than 11 in the initial state of bR[29] to 7.1 in the N state.[31] This parameter represents the basis for the understanding of unidirectional proton transfer within a protein, and the advantages offered by evanescent wave IR spectroscopy make this quantitative information possible.

4.2. Cytochrome c oxidase: A respiratory protein

Cytochrome c oxidase is the terminal enzyme in the respiratory chain of mitochondria and many bacteria.[32] It catalyzes the conversion of dioxygen to water and, in so doing, transfers four electrons from four reduced cytochrome c molecules, consumes four protons for the chemical conversion of each dioxygen molecule, and pumps four additional protons across the membrane. The net movement of charge contributes to the electrochemical gradient that is used to fuel ATP synthesis. A team of heme and copper cofactors and a series of conserved amino acids coordinate the transfer of electrons, pumping of protons, and the reduction of dioxygen. A schematic of the catalytic reactions is shown in Figure 4A with the crystallographic model of cytochrome c oxidase from *Rhodobacter sphaeroides*. Evanescent-wave IR difference spectroscopy has been used to observe structural changes occurring in transitions between three different states termed R_4, P_M, and F and the fully oxidized state O. These three intermediate states have been created by chemical composition changes of the aqueous buffer. We will focus here again on the protonation reactions occurring during electron transfer. An examination of the carbonyl region is given in Figure 4B. In this region, only vibrations of protonated carboxylic acids appear; this allows the role of a key glutamic acid E286 to be elucidated. It was demonstrated that this residue is protonated in both R_4 and O states and undergoes a change of hydrogen bonding in the transition.[33] In addition, it emerges from the difference spectra that the E286 side chain is deprotonated in P_M and

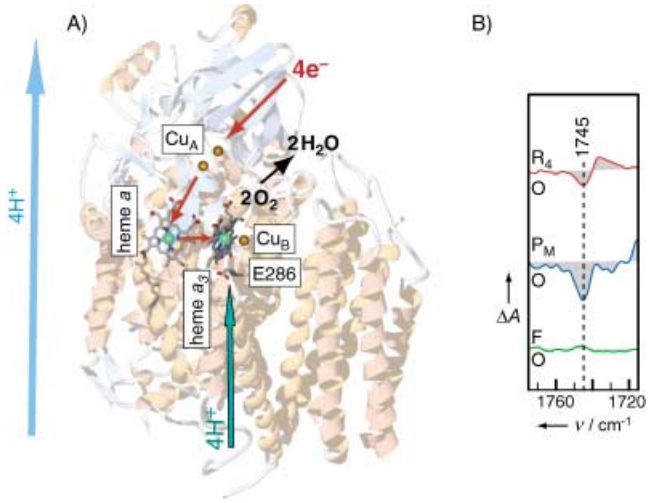

Figure 4. *A) Schematic of the respiratory membrane cytochrome c oxidase from* Rhodobacter sphaeroides *(PDB entry: 1M56) depicting some of the most essential elements of the enzymatic machinery. These elements include three copper atoms (two Cu_A and one Cu_B), and two heme cofactors (heme a and heme a_3). The catalytic task of this enzyme is the four-electron reduction of molecular oxygen to water. Electrons are passed from cytochrome c from the periplasmic side to the protein active site by the pathway shown in red arrows. Four protons are taken up from the opposite side of the membrane (green arrow) and another four protons are translocated across the whole protein (light blue arrow). Together heme a_3 and Cu_B form the active site, where molecular oxygen is bound and chemically converted to water. The residue E286 is close to this binuclear center and is involved in proton transfer to this site. B) ATR/FTIR difference spectra in the carbonyl region for different states of cytochrome c oxidase showing the $R_4 - O$ (red trace), $P_M - O$ (blue trace), and $F - O$ (green trace) differences. The dashed line indicates the frequency of the C=O stretching vibration of the carboxylic acid side chain of E286.*

unchanged, that is, remains protonated, in F.[34] Direct observation of such structural details about this key residue is only possible with the ATR/FTIR technique.

4.3. Examples from receptors: Rhodopsin and nAChR

We turn now from proteins that fuel metabolism to one whose role is processing information. Rhodopsin is a member of the family of G-protein coupled receptors (GPRCs), membrane proteins composed of seven transmembrane helices that participate in numerous signaling pathways.[35] Rhodopsin is regarded as a prototypical GPRC and it is the only one for which a highly resolved crystallographic model exists.[36] Rhodopsin's light-driven stimulus via its retinal chromophore makes it similar to bR. In contrast, however, rhodopsin's catalytic task is not creating an electrochemical gradient but rather activating the cognate cytosolic G protein transducin. The absorption of light induces structural changes in rhodopsin such that it is capable of interacting with transducin. One of the specific changes, protonation of a highly conserved carboxylic acid residue in the cytoplasmic domain of helix III, has been elucidated by evanescent-wave IR difference spectroscopy.[37, 38] IR difference spectra for the light-activated catalytic cycle were compared in the presence and absence of transducin. A comparison of the transducin-mediated changes for the wild-type and mutants of this glutamic acid residue, E134 in bovine rhodopsin, revealed that the protonation of this residue is critical to the binding of transducin to the activated form of rhodopsin (the MII state).

Another avenue to understanding the molecular mechanism of a membrane protein is examining aspects of the structural changes caused by inhibitors. Evanescent-wave IR difference spectroscopy was used to examine the molecular basis of the inhibition of suramin on rhodopsin.[39] Comparison of the IR difference spectra for rhodopsin's light-activated catalytic cycle in the absence and presence of suramin revealed that suramin does not alter the structure of rhodopsin in its intermediate states. Rather, the spectra indicate that suramin's mode of inhibition occurs through a decrease of transducin's membrane affinity, and thereby a decrease in transducin binding to rhodopsin.

Acetylcholine receptor (AChR) proteins are a family of ligand-gated ion channels that perform a central role in signal transduction across postsynaptic membranes.[40] Binding of the neurotransmitter acetylcholine causes a channel formed by the five-subunit receptor to open; this results in the influx of specific ions, usually cations, and thereby in a rapid change in the electrical and secondarily metabolic state of the cell. Nicotine is a potent agonist for nicotinic AChRs (nAChRs), that is, it has the same action as acetylcholine. In the absence of a bound ligand, the receptor can undergo a transition from its normal resting state to a desensitized state in which ligand-binding affinity is drastically reduced. Evanescent-wave IR difference spectroscopy has been used to try to link this resting-to-desensitized transition to a molecular mechanism by using a variety of ligands and lipid environments.[41] Key band features of these evanescent-wave IR difference spectra have demonstrated the involvement of tyrosine, glutamic or aspartic acid, and tryptophane side chains.[42] The results have led to a detailed model of the structural changes that modulate ligand affinities.[41] In the absence of a crystal structure, the evanescent-wave IR difference spectra have provided a considerable amount of structural information. In addition, the technique has also provided clinically relevant informational about the interactions of nAChR with local anesthetics.[43]

5. Outlook

Evanescent-wave IR difference spectroscopy is a means of deducing the role of individual amino acids in the molecular mechanism of membrane proteins. This technique shows applicability for broader use in all classes of membrane proteins. One of the major benefits of using this technique is the ease with which it can be coupled to other techniques. Evanescent-wave IR spectroscopy can be used in combination with electrochemical and rapid-mixing methods.

Surface-enhanced spectroscopy, one of the next logical advances in ATR methodology,[44] can be used to probe proteins on the level of a single monolayer. For this purpose, we have recently developed SEIDA (surface-enhanced infrared difference absorption) spectroscopy and detected electrochemically induced changes in a cytochrome c monolayer adsorbed onto a modified gold surface.[45] Gold can be functionalized by standard techniques to covalently attach virtually any protein to the metal surface. SEIDA spectroscopy represents a nanotechnological approach towards the investigation of single native membranes and the molecular changes of their constituents upon an external trigger. Even time-resolved experiments on protein monolayers, as provided by step-scan spectroscopy, are possible as recently performed in our laboratory.[46]

Keywords: attenuated total reflection spectroscopy · bacteriorhodopsin · cytochrome c oxidase · IR spectroscopy · membrane proteins · reaction mechanisms

[1] B. Selinsky, *Membrane Protein Protocols: Expression, Purification, and Crystallization*, Humana Press, Totowa, NJ, **2003**.
[2] C. Ostermeier, H. Michel, *Curr. Opin. Struct. Biol.* **1997**, *7*, 697 – 701.
[3] C. Hunte, H. Michel, *.Curr.Opin.Struct.Biol.* **2002**, *12*, 503 – 508.
[4] P. Nollert, J. Navarro, E. M. Landau, *Methods Enzymol.* **2002**, *343*, 183 – 199.
[5] K. Gerwert, *Curr. Opin. Struct. Biol.* **1993**, *3*, 769 – 773.
[6] W. Mäntele, *Trends Biochem. Sci.* **1993**, *18*, 197 – 202.
[7] R. Vogel, F. Siebert, *Curr. Opin. Chem. Biol.* **2000**, *4*, 518 – 523.
[8] C. Zscherp, A. Barth, *Biochemistry* **2001**, *40*, 1875 – 1883.
[9] A. K. Dioumaev, Biochemistry **2001**, *66*, 1269 – 1276.
[10] A. Barth, *Prog. Biophys. Mol. Biol.* **2000**, *74*, 141 – 173.
[11] M. Engelhard, K. Gerwert, B. Hess, W. Kreutz, F. Siebert, *Biochemistry* **1985**, *24*, 400 – 407.
[12] R. Hienerwadel, A. Boussac, J. Breton, B. A. Diner, C. Berthomieu, *Biochemistry* **1997**, *36*, 14712 – 14723.
[13] C. Berthomieu, R. Hienerwadel, A. Boussac, J. Breton, B. A. Diner, *Biochemistry* **1998**, *37*, 10547 – 10554.
[14] N. J. Harrick, *Internal Reflection Spectroscopy*, Wiley, New York, **1967**.
[15] U. P. Fringeli, H. H. Günthard in *Membrane Spectroscopy* (Ed.: E. Grell), Springer, New York, **1981**, pp. 270 – 332.
[16] E. Goormaghtigh, V. Raussens, J. M. Ruysschaert, *Biochim. Biophys. Acta* **1999**, *1422*, 105 – 185.
[17] J. Heberle, C. Zscherp, *Appl. Spectrosc.* **1996**, *50*, 588 – 596.
[18] L. K. Tamm, S. A. Tatulian, *Q. Rev. Biophys.* **1997**, *30*, 365 – 429.

[19] S. Terrettaz, W. P. Ulrich, H. Vogel, Q. Hong, L. G. Dover, J. H. Lakey, *Protein Sci.* **2002**, *11*, 1917 – 1925.
[20] P. W. Bohn, *Annu. Rev. Mater. Sci.* **1997**, *27*, 469 – 498.
[21] W. Suetaka, J. T. Yates, *Surface Infrared and Raman Spectroscopy: Methods and Applications*, Plenum, New York, **1995**.
[22] J. T. Yates, T. E. Madey, *Vibrational Spectroscopies of Molecules on Surfaces*, Plenum, New York, **1995**.
[23] J. L. Rigaud, D. Levy, G. Mosser, O. Lambert, *Eur. Biophys. J.* **1998**, *27*, 305 – 319.
[24] J. Heberle, *Biochim. Biophys. Acta* **2000**, *1458*, 135 – 147.
[25] C. Zscherp, J. Heberle, *J. Phys. Chem. B* **1997**, *101*, 10542 – 10547.
[26] O. Weidlich, F. Siebert, *Appl. Spectrosc.* **1993**, *47*, 1394 – 1400.
[27] M. S. Braiman, K. J. Rothschild, *Annu. Rev. Biophys. Biophys. Chem.* **1988**, *17*, 541 – 570.
[28] K. Gerwert, G. Souvignier, B. Hess, *Proc. Natl. Acad. Sci. USA* **1990**, *87*, 9774 – 9778.
[29] S. Száraz, D. Oesterhelt, P. Ormos, *Biophys. J.* **1994**, *67*, 1706 – 1712.
[30] T. Friedrich, S. Geibel, R. Kalmbach, I. Chizhov, K. Ataka, J. Heberle, M. Engelhard, E. Bamberg, *J. Mol. Biol.* **2002**, *321*, 821 – 838.
[31] C. Zscherp, R. Schlesinger, J. Tittor, D. Oesterhelt, J. Heberle, *Proc. Natl. Acad. Sci. USA* **1999**, *96*, 5498 – 5503.
[32] G. T. Babcock, M. Wikström, *Nature* **1992**, *356*, 301 – 309.
[33] R. M. Nyquist, D. Heitbrink, C. Bolwien, T. A. Wells, R. B. Gennis, J. Heberle, *FEBS Lett.* **2001**, *505*, 63 – 67.
[34] R. M. Nyquist, D. Heitbrink, C. Bolwien, R. B. Gennis, J. Heberle, *Proc. Natl. Acad. Sci. USA* **2003**, *100*, 8715 – 8720.
[35] H. Schwalbe, G. Wess, *ChemBioChem* **2002**, *3*, 915 – 919.
[36] T. Okada, K. Palczewski, *Curr. Opin. Struct. Biol.* **2001**, *11*, 420 – 426.
[37] K. Fahmy, T. P. Sakmar, F. Siebert, *Biochemistry* **2000**, *39*, 10607 – 10612.
[38] K. Fahmy, *Biophys. J.* **1998**, *75*, 1306 – 1318.
[39] N. Lehmann, A. G. Krishna, K. Fahmy, *Biophys. J.* **2002**, *82*, 793 – 802.
[40] A. Karlin, *Nat. Rev. Neurosci.* **2002**, *3*, 102 – 114.
[41] S. E. Ryan, D. G. Hill, J. E. Baenziger, *J. Biol. Chem.* **2002**, *277*, 10420 – 10426.
[42] J. E. Baenziger, K. W. Miller, K. J. Rothschild, *Biochemistry* **1993**, *32*, 5448 – 5454.
[43] S. E. Ryan, J. E. Baenziger, *Mol. Pharmacol.* **1999**, *55*, 348 – 355.
[44] M. Osawa, *Bull. Chem. Soc. Jpn.* **1997**, *70*, 2861 – 2880.
[45] K. Ataka, J. Heberle, *J. Am. Chem. Soc.* **2003**, *125*, 4986 – 4987.
[46] K. Ataka, J. Heberle, unpublished results.

Received: June 11, 2003
Revised: January 15, 2004 [C687]

